第 35 卷第 11 期
2019 年 11 月

无 机 化 学 学 报
CHINESE JOURNAL OF INORGANIC CHEMISTRY

Vol.35 No.11
2145-2151

2,6-二(1-咪唑基)萘和二羧酸构筑的金属–有机框架化合物：合成、晶体结构和荧光识别性能

刘志强[1,2] 曹师虎[1] 张 哲[1] 武峻峰[1] 赵 越[2] 孙为银*[,2]

([1]安庆师范大学化学化工学院,光电磁功能材料安徽省重点实验室,光电磁功能配合物和纳米配合物安徽省重点实验室,安庆 246011)

([2]南京大学化学化工学院,配位化学国家重点实验室,南京 210023)

摘要：利用 2,6-二(1-咪唑基)萘(L)和二羧酸配体与过渡金属盐反应,通过溶剂热法合成了 3 个新颖的金属有机框架化合物(MOFs):[Co(L)(AIP)]·2DMF (**1**),[Co(L)(AIP)]·DMF (**2**)和[Co(L)(IDC)(H_2O)$_2$]·0.5L·H_2O (**3**)(H_2AIP=5-氨基间苯二甲酸,H_2IDC=4,4′-亚氨基二苯甲酸)。利用元素分析、红外、X 射线单晶和粉末衍射、热重分析等对 MOFs 进行了表征。单晶结构解析结果表明:**1** 属于单斜晶系 *C*2/*c* 空间群,**2** 和 **3** 属于三斜晶系 $P\bar{1}$ 空间群。**1** 和 **3** 均为一维的链状结构,**2** 为二维的层状结构,三者通过氢键作用形成三维超分子结构。此外,对 MOFs 的热稳定性和荧光性质进行了研究,发现 **3** 通过荧光猝灭对丙酮分子具有识别作用。

关键词：金属–有机框架化合物；2,6-二(1-咪唑基)萘；晶体结构；荧光性质

中图分类号：O614.81+2 **文献标识码**：A **文章编号**：1001-4861(2019)11-2145-07

DOI:10.11862/CJIC.2019.225

Metal-Organic Frameworks with 2,6-Di(1*H*-imidazol-1-yl)naphthalene and Dicarboxylate Ligands: Synthesis, Crystal Structure and Photoluminescence Sensing Property

LIU Zhi-Qiang[1,2] CAO Shi-Hu[1] ZHANG Zhe[1] WU Jun-Feng[1] ZHAO Yue[2] SUN Wei-Yin*[,2]

([1]*School of Chemistry and Chemical Engineering, Anhui Province Key Laboratory of Functional Optical, Electrical and Magnetic Materials, Key Laboratory of Functional Coordination Compounds and Nano Materials of Anhui Higher Education Institutes, Anqing Normal University, Anqing, Anhui* 246011, *China*)

([2]*State Key Laboratory of Coordination Chemistry, School of Chemistry and Chemical Engineering, Nanjing University, Nanjing* 210023, *China*)

Abstract: Reactions of 2,6-di(1*H*-imidazol-1-yl)naphthalene (L) and dicarboxylic acid ligands with corresponding metal salts under solvothermal conditions gave rise to three new metal-organic frameworks (MOFs) [Co(L)(AIP)]·2DMF (**1**),[Co(L)(AIP)]·DMF (**2**) and [Co(L)(IDC)(H_2O)$_2$]·0.5L·H_2O (**3**) (H_2AIP=5-aminoisophthalic acid,H_2IDC=4,4′-iminodibenzoic acid). The MOFs have been structurally characterized by single-crystal and powder X-ray diffraction analyses, elemental analyses, infrared spectra (IR) and thermogravimetric analysis (TGA). MOF **1** crystallizes in monoclinic space group *C*2/*c*, while **2** and **3** are triclinic space group $P\bar{1}$. MOFs **1** and **3** have distinct infinite one-dimensional (1D) chain structures, and **2** is a two-dimensional (2D) network, which are

收稿日期:2019-08-28。收修改稿日期:2019-09-11。

安徽省自然科学基金(No.1908085QB47),安徽高校自然科学研究重点项目(No.KJ2018A0371)和配位化学国家重点实验室开放课题(No.SKLCC1906)资助。

*通信联系人。E-mail:sunwy@nju.edu.cn;会员登记号:S060015599P。

further linked together by hydrogen bonding interactions to give the eventual three-dimensional (3D) supramolecular architectures. Furthermore, the thermal stability and photoluminescence property of the MOFs were investigated, and it was found that **3** can efficiently detect acetone molecules via fluorescent quenching. CCDC: 1949785, **1**; 1949786, **2**; 1949787, **3**.

Keywords: metal-organic frameworks; 2,6-di(1*H*-imidazol-1-yl)naphthalene; crystal structure; photoluminescence property

0 Introduction

The research field of metal-organic frameworks (MOFs) has undergone rapid development in the past decade. Benefiting from their fascinating structures, large surface areas, tunable pore size and abundant active sites, MOFs have been extensively investigated in the fields of gas adsorption/separation, magnetism, sensing and detection, catalysis and so on[1-11]. Despite the great progress achieved, it is still remarkable challenge for fabrication of desired MOFs, since the formation of MOFs can be affected by varied factors including the nature of organic ligand and metal center, reaction conditions such pH, solvent and temperature. Our previous studies have shown that organic compounds with 1*H*-imidazol-1-yl groups are versatile ligands for the construction of MOFs with definite structures and properties [12-16]. On the other hand, with the rapid development of industry and the social activities of human beings, the efficient detection of small organic molecules is important in the environmental and biological systems[17-20].

Based on the above mentioned background, we focused our attention on reactions of a new designed bis(1*H*-imidazol-1-yl) ligand 2,6-di(1*H*-imidazol-1-yl) naphthalene (L) and Co(Ⅱ) salts with different dicarboxylic acids. In this work, three new MOFs [Co(L)(AIP)]·2DMF (**1**), [Co(L)(AIP)]·DMF (**2**) and [Co(L)(IDC)$(H_2O)_2$]·0.5L·H_2O (**3**) (H_2AIP=5-aminoisophthalic acid, H_2IDC=4,4′-iminodibenzoic acid, DMF=*N*,*N*-dimethylformamide) were successfully synthesized. The MOFs were characterized by X-ray crystallography, IR spectroscopy, elemental and thermal analyses. In addition, luminescence studies reveal that MOF **3** is a responsive luminescent probe for detecting acetone molecules.

1 Experimental

1.1 Materials and methods

All commercially available chemicals and solvents are of reagent grade and were used as received without further purification. Ligand L was synthesized by similar method reported in the literature[21]. FT-IR spectra were recorded in a range of 400~4 000 cm^{-1} on a Bruker Vector 22 FT-IR spectrometer using KBr pellets. Thermogravimetric analysis (TGA) was performed on a Mettler-Toledo (TGA/DSC1) thermal analyzer under nitrogen atmosphere with a heating rate of 10 ℃·min^{-1}. Powder X-ray diffraction (PXRD) patterns were obtained on a Bruker D8 Advance diffractometer using Cu $K\alpha$ (λ=0.154 18 nm) in 2θ range of 5°~50° at 293 K, in which the X-ray tube was operated at 40 kV and 40 mA. Photoluminescence spectra were measured on an Aminco Bowman Series 2 spectrofluorometer with a xenon arc lamp as the light source. In the measurements of emission and excitation spectra, the pass width was 5 nm.

1.2 Synthesis of MOFs 1~3

1.2.1 Synthesis of **1**

A mixture of L (14.3 mg, 0.05 mmol), $Co(NO_3)_2$·$6H_2O$ (29.1 mg, 0.1 mmol) and H_2AIP (9.1 mg, 0.05 mmol) in DMF/H_2O (10 mL, 3∶1, *V*/*V*) was sealed in a glass vial and heated at 90 ℃ for 3 days. The resulting purple block crystals were collected in 81% yield based on L. Elemental analysis Calcd. for $C_{30}H_{31}N_7O_6Co$ (%): C 55.90, H 4.85, N 15.21; Found(%): C 55.62, H 4.93, N 15.29. Selected IR peaks (cm^{-1}, Fig.S1 in Supporting information): 3 443 (w), 3 138 (w), 2 883 (w), 1 665 (s), 1 576 (s), 1 510 (m), 1 352 (s), 1 253 (s), 1 098 (m), 986 (m), 946 (m), 733 (m), 611 (m), 504 (w).

1.2.2 Synthesis of **2**

MOF **2** was obtained by the same procedure as

that used for preparation of **1**, except that DMF/H_2O (10 mL, 1:3, *V*/*V*) was used instead of DMF/H_2O (10 mL, 3:1, *V*/*V*). After being cooled to room temperature, pink block crystals of **2** were isolated in 58% yield based on L. Elemental analysis Calcd. for $C_{27}H_{24}N_6O_5Co$ (%): C 56.75, H 4.23, N 14.71; Found(%): C 56.67, H 4.31, N 14.75. Selected IR peaks (cm^{-1}, Fig.S1): 3 335 (m), 2 918 (w), 1 672 (s), 1 586 (s), 1 436 (m), 1 388 (s), 1 247 (s), 1 056 (m), 932 (m), 831 (s), 792 (s), 720 (s), 615 (m).

1.2.3 Synthesis of **3**

MOF **3** was achieved by the same procedure used for preparation of **2**, except that H_2IDC (12.9 mg, 0.05 mmol) was used instead of H_2AIP. After being cooled to room temperature, pink block crystals of **3** were isolated in 76% yield based on L. Elemental analysis Calcd. for $C_{38}H_{33}N_7O_7Co$ (%): C 60.16, H 4.38, N 12.92; Found(%): C 60.09, H 4.43, N 12.89. Selected IR peaks (cm^{-1}, Fig.S1): 3 408 (m), 3 139 (m), 1 597 (s), 1 506 (s), 1 372 (s), 1 311 (s), 1 110 (w), 1 053 (m), 928 (w), 813 (w), 730 (w), 653 (m), 474 (w).

1.3 Crystallographic data collection and refinement

Crystallographic data for **1~3** were collected on a Bruker Smart Apex Ⅱ CCD with graphite monochromated Mo *Kα* radiation source (λ=0.071 073 nm). The integration of the diffraction data as well as the intensity corrections for the Lorentz and polarization effects were carried out using the SAINT program[22]. Semi-empirical absorption correction was applied using SADABS program[23]. The structures of **1~3** were determined by direct methods and refined anisotropically on F^2 by the full-matrix least-squares technique with SHELXTL-2016 program package[24-25]. The hydrogen atoms except for those of water molecules were generated geometrically and refined isotropically using the riding model. The crystal data and structure refinements for the MOFs are listed in Table 1. Selected bond lengths and angles are listed in Table S1, and the hydrogen bonding data are given in Table S2.

CCDC: 1949785, **1**; 1949786, **2**; 1949787, **3**.

Table 1 Crystal data and structure refinements for complexes 1~3

Complex	1	2	3
Empirical formula	$C_{30}H_{31}N_7O_6Co$	$C_{27}H_{24}N_6O_5Co$	$C_{38}H_{33}N_7O_7Co$
Formula weight	644.55	571.45	758.64
Crystal system	Monoclinic	Triclinic	Triclinic
Space group	*C*2/*c*	$P\bar{1}$	$P\bar{1}$
a / nm	1.012 0(2)	1.006 04(9)	1.166 43(8)
b / nm	2.050 9(4)	1.102 61(10)	1.175 44(8)
c / nm	1.525 7(3)	1.295 70(12)	1.279 95(8)
α / (°)		66.862(1)	76.460(1)
β / (°)	108.012(3)	72.915(1)	84.218(1)
γ / (°)		80.548(1)	80.201(1)
V / nm^3	3.011 4(10)	1.261 4(2)	1.677 83(19)
Z	4	2	2
D_c /(g·cm^{-3})	1.422	1.505	1.502
μ / mm^{-1}	0.625	0.732	0.576
F(000)	1 340	590	786
Reflection collected	10 339	8 742	10 803
Unique reflection	3 478	5 769	6 885
Goodness-of-fit	1.020	0.866	0.844
R_1[a] [$I>2\sigma(I)$]	0.044 5	0.035 7	0.040 8
wR_2[b] [$I>2\sigma(I)$]	0.142 3	0.118 9	0.131 0

[a] $R_1=\sum||F_o|-|F_c||/\sum|F_o|$; [b] $wR_2=|\sum w(|F_o|^2-|F_c|^2)|/\sum|w(F_o)^2|^{1/2}$, where $w=1/[\sigma^2(F_o^2)+(aP)^2+bP]$, $P=(F_o^2+2F_c^2)/3$.

2 Results and discussion

2.1 Crystal structures of 1~3

2.1.1 Crystal structure of **1**

The single-crystal X-ray diffraction analysis revealed that MOF **1** crystallizes in monoclinic *C*2/*c* space group. The asymmetric unit contains half molecule of [Co(L)(AIP)]·2DMF, namely one Co(Ⅱ) located at specific position with site occupancy of 0.5, half L, half deprotonated AIP^{2-} and one free DMF molecule. As exhibited in Fig.1a, Co1 is four-coordinated by two N atoms (N1, N1A) from two different L and two carboxylate O ones (O1, O1A) from two distinct AIP^{2-} ligands, forming a distorted $\{CoO_2N_2\}$ tetrahedral coordination geometry. The Co-N and Co-O bond lengths are 0.203 29(19) and 0.198 37(15) nm, respectively. The coordination angles around Co1 are from 96.41(9)° to 118.25(7)° (Table S1). It is noteworthy that each L links two Co(Ⅱ) to form an infinite 1D zigzag chain (Fig.1b), and each AIP^{2-} connects two Co(Ⅱ) using its two carboxylate groups each with $(\mu_1\text{-}\eta^1\text{:}\eta^0)\text{-}(\mu_1\text{-}\eta^1\text{:}\eta^0)$-$AIP^{2-}$ coordination mode (Scheme 1a) to give another 1D chain (Fig.1c). Then, two kinds of 1D chains cross-link together via the coordination of Co(Ⅱ) to generate a 1D chain of **1** (Fig.1d), which is further extended into a 3D supramolecular architecture through O–H⋯O and N–H⋯O hydrogen bonding interactions (Fig.1e and Table S2).

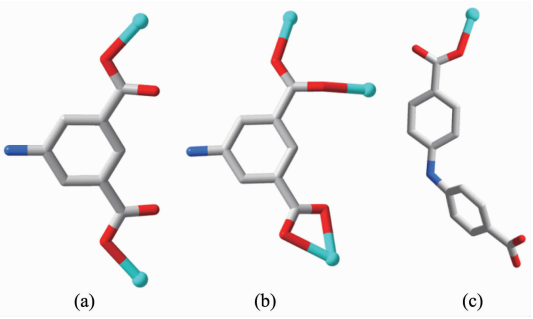

Scheme 1 Coordination modes of AIP^{2-} and IDC^{2-} in **1~3**

2.1.2 Crystal structure of **2**

MOF **2** was isolated under the same conditions as **1**, except the change of volume ratio of DMF and H_2O. The X-ray diffraction analysis indicates that MOF **2** crystallizes in triclinic $P\bar{1}$ space group. There are one Co(Ⅱ), one L, one completely deprotonated AIP^{2-} and one free DMF molecule in the asymmetric unit of **2**. As shown in Fig.2a, Co1 is six coordinated with seriously distorted octahedral coordination geometry. In addition, the Co(Ⅱ) ions in **1** have N_2O_2 coordination environments (Fig.1a), while the ones in **2** are surrounded by N_2O_4 donor sets (Fig.2a). On the other hand, the AIP^{2-} adopts a μ_3-bridging mode to connect three metal ions using its two carboxylate groups with

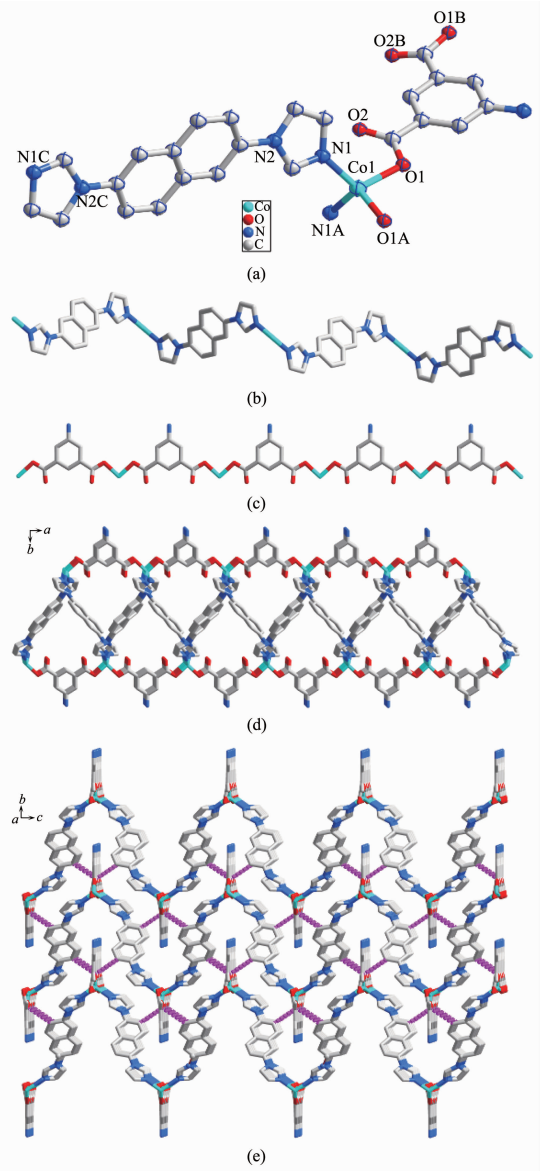

Hydrogen atoms and free solvent molecules are omitted for clarity; Symmetry codes: A: –*x*, *y*, –*z*+1/2; B: –*x*+1, *y*, –*z*+1/2

Fig.1 (a) Coordination environment of Co(Ⅱ) in **1** with the ellipsoids drawn at 30% probability level; (b) 1D chain of Co(Ⅱ)-L in **1**; (c) 1D chain of Co(Ⅱ)-AIP^{2-} in **1**; (d) 1D chain of **1**; (e) 3D structure of **1** with hydrogen bonds indicated by dashed lines

(μ_1-η^1:η^1)-(μ_2-η^1:η^1)-AIP coordination mode (Scheme 1b). Ligands AIP^{2-} link Co(Ⅱ) ions to form a 1D chain (Fig.2b). The Co(Ⅱ)-AIP^{2-} 1D chains are further connected by Co(Ⅱ)-L 1D chain (Fig.2c) to generate a 2D network (Fig.2d), which is further extended into a 3D supramolecular architecture through hydrogen bonding interactions (Fig.2e and Table S2).

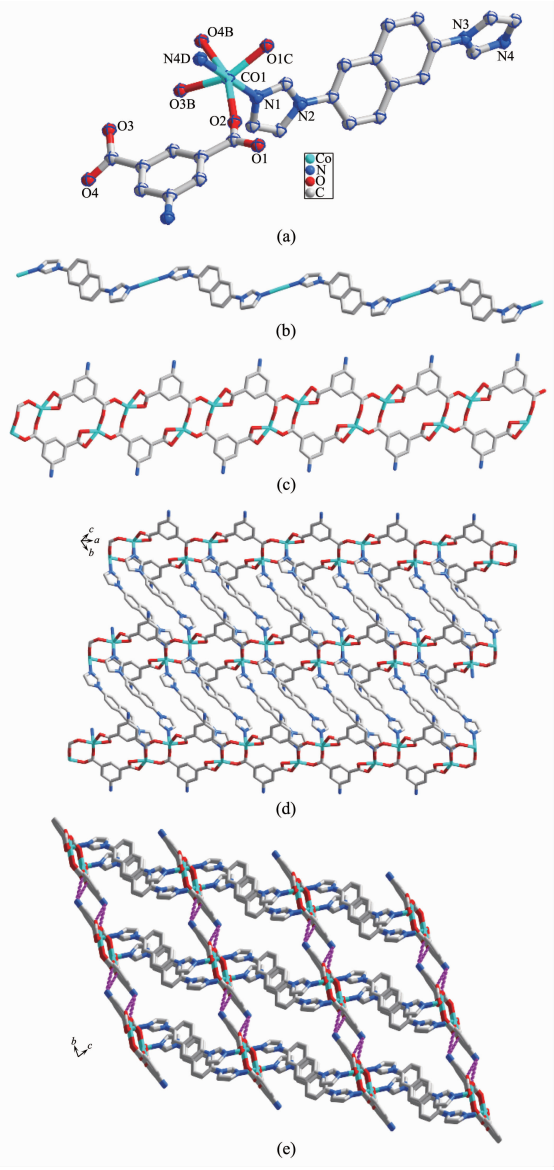

Hydrogen atoms and free DMF molecules are omitted for clarity; Symmetry codes: B: $-x$, $-y$, $-z+2$; C: $-x+1$, $-y+1$, $-z+2$; D: x, $y+1$, z

Fig.2 (a) Coordination environment of Co(Ⅱ) in **2** with the ellipsoids drawn at 30% probability level; (b) 1D chain of Co(Ⅱ)-L in **2**; (c) 1D chain of Co(Ⅱ)-AIP^{2-} in **2**; (d) 2D network of **2**; (e) 3D structure of **2** with hydrogen bonds indicated by dashed lines

2.1.3 Crystal structure of **3**

When H_2IDC instead of H_2AIP was used under the same reaction conditions as those for preparation of **2**, MOF **3** was generated. As illustrated in Fig.3a, Co1 ion is six-coordinated with distorted octahedral coordination geometry surrounded by two nitrogen atoms (N1, N4A) from two different L and three oxygen ones (O5, O5D, O6) from coordinated aqua molecules

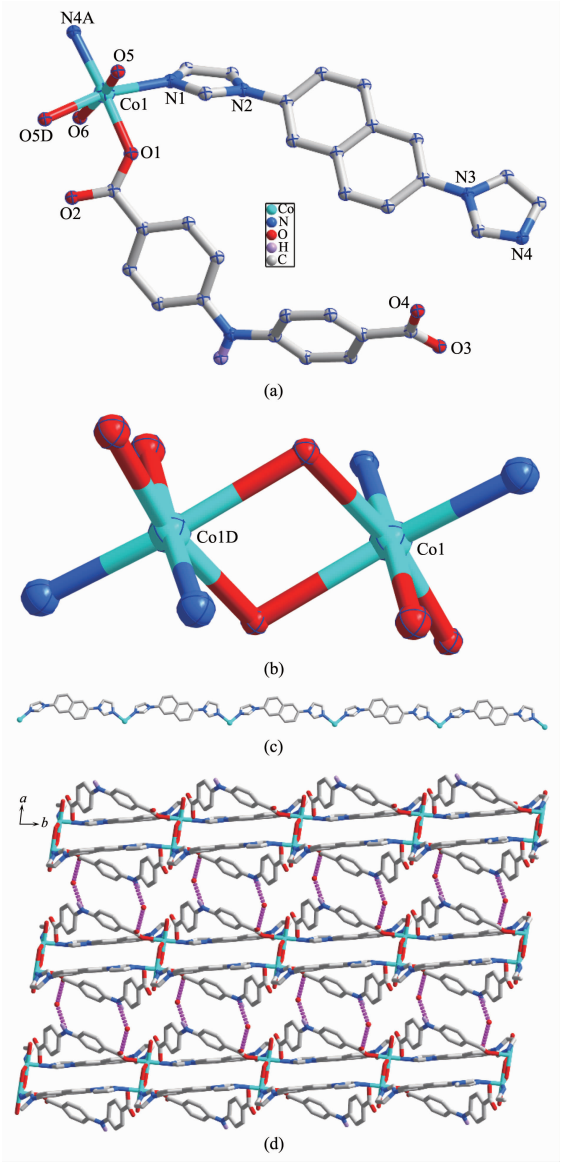

Hydrogen atoms and free water and L molecules are omitted for clarity; Symmetry codes: A: x, $y+1$, $z-1$; D: $-x$, $-y+2$, $-z$

Fig.3 (a) Coordination environment of Co(Ⅱ) in **3** with the ellipsoids drawn at 30% probability level; (b) Dinuclear SBU in **3**; (c) 1D chain constructed by Co(Ⅱ) and L; (d) 3D structure of **3** with hydrogen bonds indicated by dashed lines

and another carboxylate oxygen (O1) from IDC^{2-}. It can be seen that Co1 and Co1D are connected together through two coordinated aqua molecules to form a dinuclear cluster, which can be treated as a secondary building unit (SBU) (Fig.3b). The Co1-N bond lengths are 0.214 77(19) and 0.215 56(18) nm and Co1-O ones are in a range of 0.203 35(17)~0.224 37(16) nm. The range of coordination angles around Co1 is from 79.27(6)° to 176.80(7)° (Table S1). L ligands link Co (Ⅱ) ions to from an infinite 1D chain (Fig.3c). It is noteworthy that IDC^{2-} acts as a terminal ligand in a monodentate linkage mode (Scheme 1c). The 1D chains are further extended into a three-dimensional (3D) supramolecular architecture through hydrogen bonding interactions (Fig.3d and Table S2).

2.2 Powder X-ray diffraction and thermogravimetric analyses

The purity for the as-synthesized samples was ensured by PXRD measurements and the results are provided in Fig.S2. Each as-synthesized sample gave consistent PXRD pattern with the corresponding simulated one, implying the pure phase of **1**~**3**.

Thermogravimetric analyses (TGA) were employed to check the thermal stabilities of **1**~**3**, and the TG curves are given in Fig.S3. For **1**, a weight of loss of 22.36% was found before 270 ℃ due to the removal of two lattice DMF molecules (Calcd. 22.68%), and further weight loss started from about 330 ℃. Complex **2** lost its 12.12% weight in a temperature range of 30~370 °C, due to the departure of lattice DMF molecule (Calcd. 12.79%), and further weight loss was observed at about 420 ℃, corresponding to the collapse of the framework. In the case of **3**, a weight loss of 6.92% was detected in a temperature range of 30~200 ℃, which is ascribed to the loss of free and coordinated aqua molecules (Calcd. 7.16%). The framework of 3 collapsed from about 310 ℃.

2.3 Luminescent experiments

The emission spectra of MOF **3** and free ligand L were investigated at definite excitation wavelength as illuminated in Fig.S4. Intense emission was observed with a peak at 361 nm (λ_{ex}=324 nm) for L, which is assigned to $\pi^* \rightarrow \pi$ intraligand fluorescence, and **3** exhibits an emission at 362 nm (λ_{ex}=292 nm). The emissions of MOF **3** may be attributed to a joint contribution of the $\pi^* \rightarrow \pi$ intraligand transitions and charge transfer transitions between the L and Co(Ⅱ)[26-27].

To examine the effects of different small organic molecules on the luminescence of MOF **3**, a finely ground sample of **3** in different solvents, including C_2H_5OH, DMF, DMA (*N*,*N*-dimethylacetamide), CH_3OH, benzene, CH_2Cl_2, $CHCl_3$, THF, CH_3CN and acetone, were prepared and the luminescence properties were investigated. As shown in Fig.4, the stable suspension of **3** in C_2H_5OH showed the strongest emission and acetone gave the most significant quenching effect. The quenching efficiency of **3** dispersed in C_2H_5OH suspension with different amount of acetone was also investigated. As exhibited in Fig.5, a gradual decrease of the emission intensity was observed upon the increasing addition of acetone. The quenching

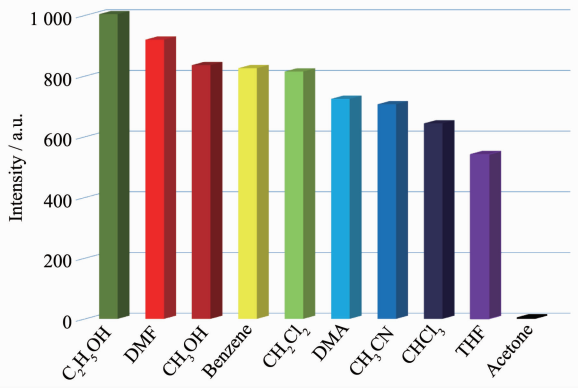

Fig.4 Photoluminescence intensities introduced into varied pure solvent upon excitation at 292 nm for **3**

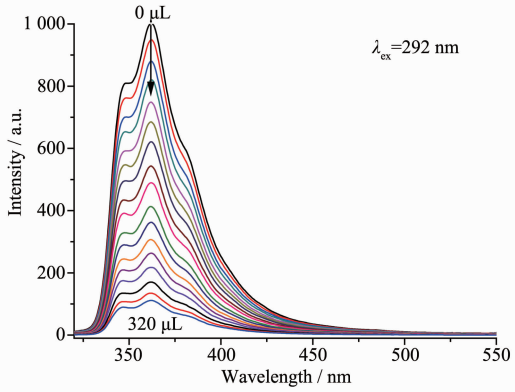

Fig.5 Photoluminescence spectra of the dispersed **3** in C_2H_5OH in the presence of varied contents of acetone solvent

behavior of the acetone molecule might be ascribed to the interaction between C=O acetone and the framework of **3**[28-30]. Thus, **3** can be considered as a potential candidate for selective sensing of acetone molecules.

3 Conclusions

In summary, three new MOFs [Co(L)(AIP)]·2DMF (**1**), [Co(L)(AIP)]·DMF (**2**) and [Co(L)(IDC)(H_2O)$_2$]·0.5L·H_2O (**3**) were successfully synthesized by using mixed ligands. MOFs **1**~**3** displayed diverse structures: **1** and **3** are 1D chains, and **2** is 2D network, which are further linked together by hydrogen bonds to give eventual 3D architectures. Furthermore, the thermal stability and photoluminescence property of the MOFs were investigated, and **3** can be regarded as candidate for the selective sensing of acetone.

Supporting information is available at http://www.wjhxxb.cn

References:

[1] Meng X, Wang H N, Song S Y, et al. *Chem. Soc. Rev.*, **2017**, **46**:464-480

[2] Wu S Y, Min H, Shi W, et al. *Adv. Mater.*, **2019**,**31**:1805871-180584

[3] Kang Y S, Lu Y, Chen K, et al. *Coord. Chem. Rev.*, **2019**,**378**:262-280

[4] Cui Y, Li B, He H, et al. *Acc. Chem. Res.*, **2016**,**49**:483-493

[5] Gu Z G, Li D J, Zheng C, et al. *Angew. Chem. Int. Ed.*, **2017**,**56**:6853-6858

[6] Cook T R, Zheng Y R, Stang P J. *Chem. Rev.*, **2013**,**113**:734-777

[7] Lustig W P, Mukherjee S, Rudd N D, et al. *Chem. Soc. Rev.*, **2017**,**46**:3242-3285

[8] Tang Q, Liu S, Liu Y, et al. *Inorg. Chem.*, **2013**,**52**:2799-2801

[9] Lin Z J, Lu J, Hong M C, et al. *Chem. Soc. Rev.*, **2014**,**43**:5867-5895

[10]Lan Y Q, Jiang H L, Li S L, et al. *Inorg. Chem.*, **2012**,**51**:7484-7491

[11]Sun Y X, Sun W Y. *CrysEngComm*, **2015**,**17**:4045-4063

[12]Su Z, Fan J, Okamura T, et al. *Cryst. Growth Des.*, **2011**,**11**:1159-1169

[13]Hua J A, Zhao Y, Kang Y S, et al. *Dalton. Trans.*, **2015**,**44**:11524-11532

[14]Li Y L, Zhao D, Zhao Y, et al. *Dalton. Trans.*, **2016**,**45**:8816-8823

[15]Deng Y, Yao Z Y, Wang P, et al. *Sens. Actuators B*: *Chem.*, **2017**,**244**:114-123

[16]Li Y L, Zhao Y, Kang Y S, et al. *Cryst. Growth Des.*, **2016**, **16**:7112-7123

[17]Lian X, Yan B. *Dalton. Trans.*, **2016**,**45**:2666-2673

[18]Yan W, Zhang C L, Chen S G, et al. *ACS Appl. Mater. Interfaces*, **2017**,**9**:1629-1634

[19]LIU Zhi-Qiang(刘志强), HUANG Yong-Qing(黄永清), SUN Wei-Yin(孙为银). *Chinese J. Inorg. Chem.*(无机化学学报), **2017**,**33**:1959-969

[20]Liu Z Q, Zhao Y, Deng Y, et al. *Sens. Actuators B*: *Chem.*, **2017**,**250**:179-188

[21]Fan J, Gan L,Kawaguchi H, et al. *Chem. Eur. J.*, **2003**,**9**:3965-3973

[22]*SAINT, Program for Data Extraction and Reduction*, Bruker AXS, Inc., Madison, WI, **2001**.

[23]Sheldrick G M. *SADABS*, University of Göttingen, Germany, **2003**.

[24]Sheldrick G M. *Acta Crystallogr. Sect. A*: *Found. Crystallogr.*, **2015**,**A71**:3-8

[25]Sheldrick G M. *Acta Crystallogr. Sect. C*: *Cryst. Struct. Commun.*, **2015**,**C71**:3-8

[26]Hu G F, Wen B, Yu Y H, et al. *Inorg. Chim. Acta*, **2013**, **402**:128-132

[27]Xiao Q Q, Song Z W, Li Y H, et al. *J. Solid State Chem.*, **2019**,**276**:331-338

[28]Liu Z Q, Zhao Y, Liu X H, et al. *Polyhedron*, **2019**,**167**:33-38

[29]Liu Z Q, Chen K, Zhao Y, et al. *Cryst. Growth Des.*, **2018**, **18**:1136-1146

[30]Liu Z Q, Zhao Y, Wang P, et al. *Dalton Trans.*, **2017**,**46**:9022-9029